Hindawi
Geofluids
Volume 2022, Article ID 6249369, 19 pages
https://doi.org/10.1155/2022/6249369

Research Article

Dynamic Evaluation of Flow Unit Based on Reservoir Evolution: A Case Study of Neogene Guantao Ng3 Formation in M Area, Gudao, Bohai Bay Basin

Ruhao Liu,[1] **Yu Sun**,[1] **Xiutian Yao**,[2] **Baiquan Yan**,[3] **Jun Ma**,[2] **Changchun Guo**,[4] **and Xinrui Wang**[1]

[1]*School of Earth Science, Northeast Petroleum University, Daqing, 163318 Heilongjiang, China*
[2]*Gudao Oil Production Plant, Shengli Oilfield Company, Sinopec, Dongying, 257000 Shandong, China*
[3]*Sanya Offshore Oil & Gas Research Institute, Northeast Petroleum University, Sanya, 572025 Hainan, China*
[4]*Exploration and Development Research Institute, Shengli Oilfield Company, Sinopec, Dongying, 257015 Shandong, China*

Correspondence should be addressed to Baiquan Yan; ybqhht@163.com

Received 22 October 2022; Revised 10 November 2022; Accepted 19 November 2022; Published 5 December 2022

Academic Editor: Bailu Teng

To clarify the dynamic evolution characteristics of reservoir flow units during water injection development, the upper member of the Neogene Guantao formation in Block M of Gudao Oilfield is taken as a case study. Based on logging data, water injection profile test data, subwell data, and production performance data, among others, the flow zone index (FZI static) was proposed as the static evaluation parameter of the flow unit. The relationship between cumulative water injection (W_T) and FZI change (△FZI) was fitted. Hence, the △FZI caused by water injection is combined with the static parameter of flow unit evaluation (FZI static) as the dynamic parameter of flow unit evaluation (FZI dynamic). The comprehensively evaluated reality of flow units in different periods is characterized by formula $(\text{FZI static}) + (\triangle\text{FZI}) = (\text{FZI dynamic})$. The study shows that as the division standard of the flow unit, the FZI has a good correlation with the test results of the water absorption profile, such as water absorption intensity and relative water injection volume. Using the FZI as the static parameter of flow unit evaluation, four types of flow units were divided as follows: type I flow unit, $\text{FZI} \geq 4.1$; type II flow unit, $4.1 > \text{FZI} \geq 2.4$; type III flow unit, $2.4 > \text{FZI} \geq 1.7$; type IV flow unit, $1.7 > \text{FZI}$. The reservoir porosity and permeability characteristics of different flow units are highly correlated. Moreover, the relative permeability curve confirms that different flow units have different seepage capacities. Though, comparing characteristic reservoir parameters in different periods, the reservoir's physical parameters became more conducive to fluid flow with the water injection development. The increase in the same water injection rate for type I and II flow units was greater than that for type III and IV flow units. Furthermore, when type I flow units were continuously distributed in a large area, high water consumption bands were formed, absorbing most of the water injection in the water injection wells. Hence, the waterflood efficiency was low. The change in different flow units was mainly controlled by the injection production well pattern and W_T. Combined with the relative change characteristics of interlayer flow units, the changes can be divided into increasing type change and decreasing type changes. Finally, according to the distribution characteristics of different flow units, oil saturation, and water flooding results, strategies for tapping the potential of the remaining oil from three aspects (plane, interlayer, and inner layer) were formulated.

1. Introduction

Studying reservoir flow units is crucial for reservoir characterization during oil and gas field development. The concept of reservoir flow unit proposed by Hearn et al. referred to a reservoir with similar petrophysical properties, which is continuous in longitudinal and transverse directions, and has an internal influence on the fluid flow [1]. Since then, scholars have carried out extensive research on reservoir flow unit. They have guided later

development and residual oil distribution prediction of oil and gas fields by the distribution mechanism of flow unit. Consequently, they have gradually formed a common understanding of two elements of flow unit: (1) similar seepage characteristics exist in a single flow unit, while different flow units have different seepage characteristics; (2) there are clear seepage barrier interfaces and seepage difference interfaces between flow units.

Currently, the most used methods for flow unit division include the flow zone index method (FZI) [2–6], interwell flow capacity index method (IFCI) [7, 8], modified stratum Lorentz plot method (SMLP) [9], fuzzy clustering method [10–21], gray system theory method [22, 23], and inhomogeneous comprehensive index method [24–27]. These methods are mostly based on the penetration of cores and the formation of the reservoir. Static parameters (e.g., porosity, permeability, mud content, throat radius, grain size median, and flooded layer interpretation results) obtained from logging and seismic data are used to divide flow units. Influenced by the instantaneity of static data, the flow units obtained only reflects the characteristics of fluid seepage capacity in the reservoir during drilling data acquisition. However, during the long-term water injection development of a sandstone reservoir, the pore structure, the permeability, the mud content, and other characteristics of reservoir changes can induce seepage difference in reservoir connectivity [28–35]; thus, the type of flow unit also changes. The dynamic characteristics of this flow unit are difficult to be evaluated using the parameters obtained from the above static data. Reservoir description runs through the process of exploration and development; from the well discovery to the last abandonment, it is repeatedly conducted in stages and rolls [36]. Flow units should reflect the change of fluid seepage characteristics in the reservoir in different periods, which plays an important guiding role in the adjustment of oil field development measures, prediction of remaining oil distribution, and deployment of encrypted wells. In current research results, many scholars have divided the types of flow units into multiple regions to better understand the differences between reservoirs. However, changes in the internal structural characteristics of reservoirs induced by water injection development are often ignored when dividing the flow units. However, there is still little research on changes in the types of flow units. Therefore, the dynamic characteristics of reservoir flow units in different periods of oilfield development should be studied.

This study considered the upper section of the river facies reservoir of Guantao formation in area M of the Gudao Oilfield as a case study, using enormous static and dynamic data accumulated during oil field development. The relationship between the $\triangle$FZI and water injection volume was established. The research method combining dynamic and static changes of the reservoir flow unit was discussed to promote the transition from transient characteristics of the reservoir flow unit to realistic characteristics of the reservoir flow unit. Furthermore, the dynamic evolution law of reservoir flow units in different periods during oilfield development was clarified to guide the adjustment of oil field development measures and prediction of remaining oil distribution.

2. Geological Background

Area M of the Gudao Oilfield is located in the Gudao low uplift of the Jiyang depression (Figures 1(a) and 1(b)). The upper member of the Neogene Guantao formation is a set of important oil-bearing series in the work area (Figure 1(c)). It is mainly composed of meandering river facies deposition and develops versed microfacies, such as riverbed retention deposition, edge beach, abandoned river channel, and natural embankment. Moreover, the lithology is mainly interbedded with medium fine sandstone, siltstone and grayish green, and purplish red mudstone. The reservoir has good physical properties, a porosity of 25.1%-35.6%, permeability of $544 - 1430 \times 10^{-3}\ \mu m^2$, and strong reservoir heterogeneity. The upper member of Guantao formation is divided into five sand groups (Ng5-Ng1 from bottom to top), of which Ng3 and Ng4 sand groups are the main oil-bearing series. Furthermore, the NG3 sand group is further divided into five small layers (Ng35-Ng31 from bottom to top), and the Ng4 sand group is further divided into four small layers (Ng44-Ng41 from bottom to top). Ng35 sublayer and Ng44 sublayer are the main oil-bearing reservoirs, with a thickness of about 7 ~ 13 m. The interlayer is stably developed, with a thickness of 1-5 m. Ng35 sublayer and Ng44 sublayer are independent development units [37, 38] (Figure 1(c)).

There are 127 wells within 6.4 km^2 of the study area. Since 1976, the work area has implemented the combined production of two layers of an inverted nine-point-well pattern. In 1983, it was initially densified. However, since 1990, it has been densified, opposite the row and column well pattern. The injection production streamline angles of the upper and lower system well patterns greatly differ. The upper system adopts a 30° north by west row well pattern, and the lower system adopts a 10° north by east row well pattern. After over 40 years of development, it has entered the late stage of ultrahigh water cut development. In 2017, researchers conducted layer series for well pattern exchange, with the overall streamline changed by 40°, regarding large difference in water injection distribution and uneven crude oil production in the region. After the exchange, certain development achievements were achieved. Nevertheless, problems remain, such as unclear reservoir characteristics and uncertain extreme water consumption areas. Therefore, it is important to study the change of reservoir flow unit under long-term water injection development in the study area. After more than 40 years of development, the well pattern density in the study area is large (the average well spacing is less than 200 m), and the logging data is complete. Moreover, a wealth of continuous time dynamic data has been accumulated, such as injection pressure, instantaneous water injection, cumulative water injection, and cumulative liquid production that have been accumulated. There are 18 wells with water injection profiles of test data in different

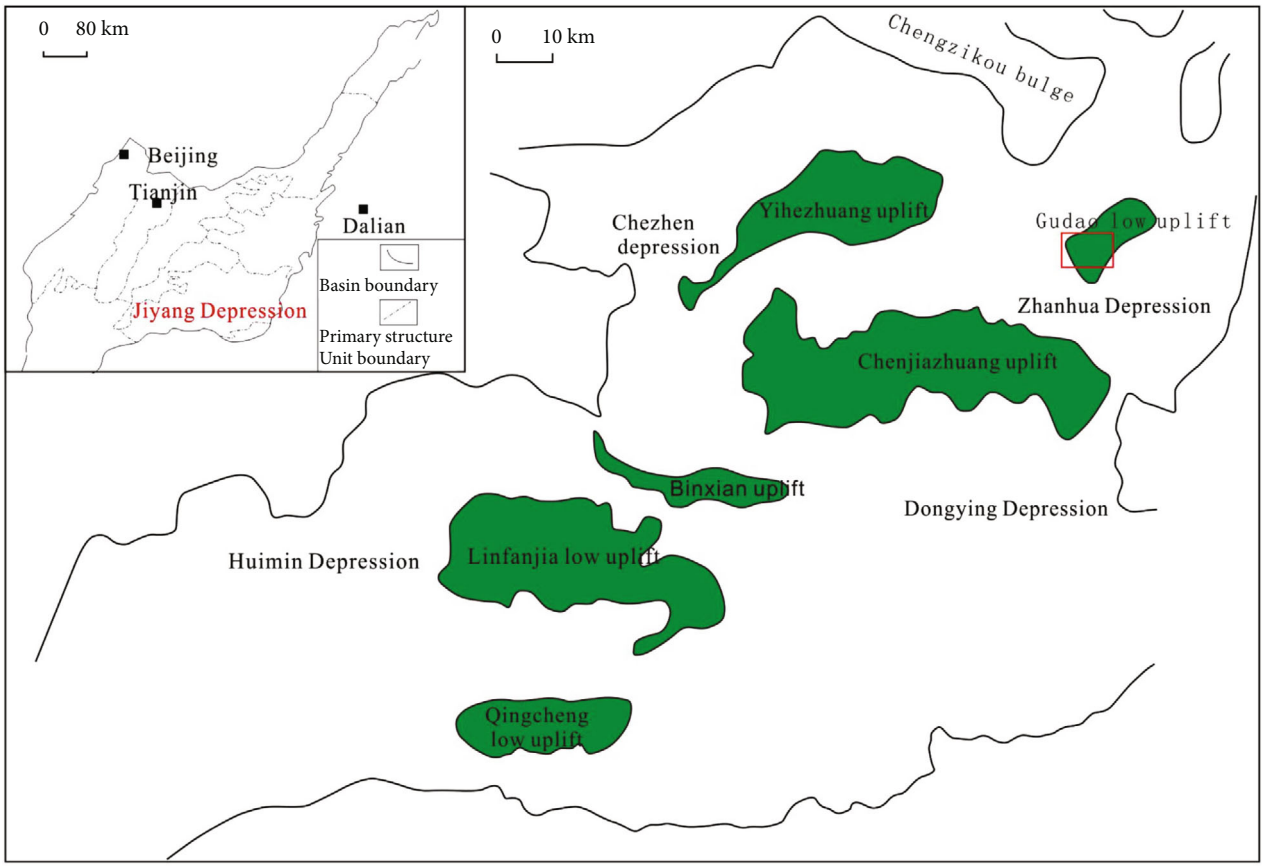

(a)

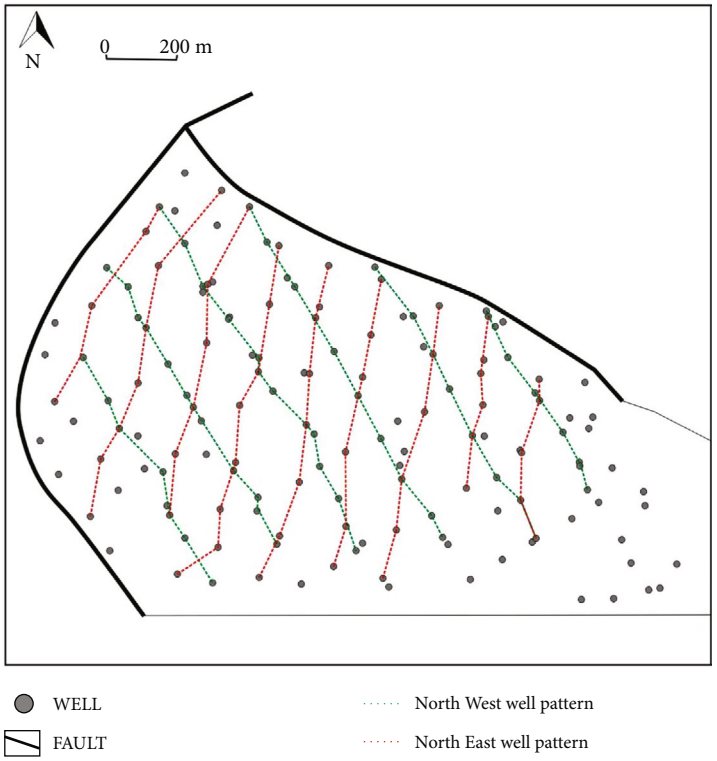

(b)

Figure 1: Continued.

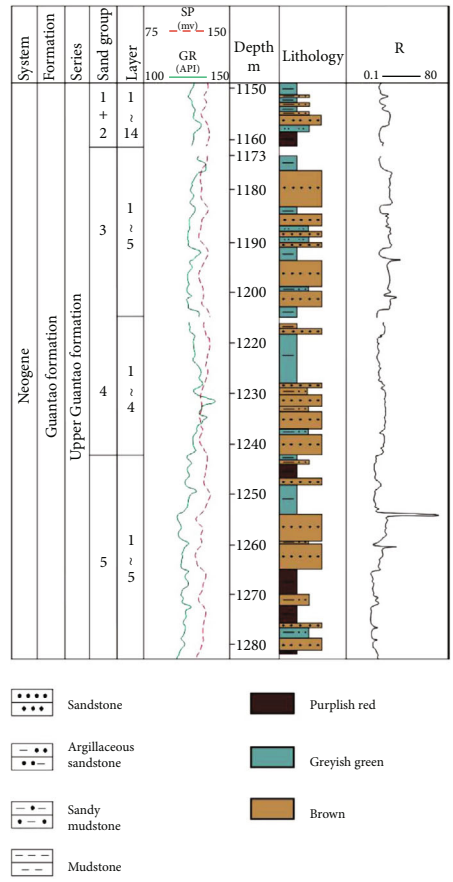

(c)

Figure 1: Stratigraphic system and regional location in the north of region M of the Gudao Oilfield. (a) Location of the study area. (b) Well pattern in the study area. (c) Comprehensive histogram of the upper member of Neogene Guantao formation in Gudao Oilfield.

periods and eight groups of subwells in different periods (well spacing is about 10–48 m). These data can provide data conditions for studying the dynamic change characteristics of flow units during water injection development.

3. Methods

To clarify the characteristics of reservoir changes in different periods, this study proposed taking the FZI (FZI static) as the static evaluation parameter of the flow unit based on logging data, water injection profile of test data, subwell data, and production performance data. The relationship between the W_T and the change in the FZI ($\triangle$FZI) was fitted through the subwells drilled in different periods. The $\triangle$FZI induced by the water injection volume was combined with the static parameter (FZI static) of the flow unit evaluation as the dynamic parameter (FZI dynamic) of the flow unit evaluation, and the two are combined to achieve a comprehensive evaluation to comprehensively evaluate the reality of the flow unit in different periods.

3.1. Evaluation of Dynamic and Static Flow Unit. Flow unit, the criterion for fluid flow capacity in the reservoir, changed with time, water injection, and other factors. Therefore, in this study, the parameters of the flow unit are divided into static and dynamic parameters to comprehensively evaluate the flow unit in different periods.

3.1.1. Static Parameters of Flow Unit Evaluation. The FZI method identified the complex changes of pore geometry in different lithofacies through core data. It then achieved the classification of flow units according to the characteristics of reservoir porosity and permeability. This method has a wide range of practicability. Compared with the gray system theory method and fuzzy clustering method, which must be comprehensively distinguished by water flooding interpretation results, this method optimally reflects the instantaneous characteristics of the reservoir. Through the previous experimental analysis and research [39–43], the change of reservoir characteristics induced by water injection development can be intuitively reflected in the change of reservoir porosity and permeability. The selection of this parameter provides a basis for studying the dynamic parameters of subsequent flow units. The static parameters of the flow unit in this study adopted the flow

zone index (FZI) proposed by Shi Wang et al. [19]. Formula (1) shows the calculation formula.

$$\mathrm{FZI}_{\mathrm{static}} = \frac{\left[0.0314(K/\Phi)^{0.5}\right]}{[\Phi/1-\Phi]}. \quad (1)$$

Formula:

(i) *FZI (static)*. The flow zone index calculated by static parameters, dimensionless

(ii) *K*. The permeability ($\times 10^{-3}\,\mu\mathrm{m}^2$)

(iii) Φ. The effective porosity (%)

Due to the existence of random error in the exponential division of flow units in the flow zone, the FZI of the same flow unit was distributed around its real mean value which is a straight-line segment on the FZI probability accumulation diagram. When there were multiple heterogeneous flow units, the FZI normal distribution was the superposition of several normal distributions. Hence, it is represented as multiple straight-line segments on the probability diagram [22]. FZI probability accumulation curve was prepared for the study area, and four divisions of flow units were provided (Figure 2): type I flow unit, FZI ≥ 4.1; type II flow unit, 4.1 > FZI ≥ 2.4; type III flow unit, 2.4 > FZI ≥ 1.7; type IV flow unit, 1.7 > FZI. Type I and II flow units were dominated by fine sandstone, type III flow units were dominated by fine siltstone, and type IV flow units were dominated by siltstone containing fine sand. Different types of flow units have different lithological types.

According to the porosity permeability curves of different types of flow units, the core porosity and permeability characteristics of different flow units had high correlation coefficients (Figure 3). Therefore, this method could effectively describe the complex characteristics of high porosity and high permeability reservoirs in this area.

Combined with the type of reservoir flow unit identified by flow zone index, the coring wells were divided into flow unit types. From the bottom-up, the quality of the flow unit gradually changes following the characteristics of porosity and permeability tested by core analysis (Figure 4). The higher the level of the flow unit, the higher the oil displacement efficiency. Therefore, the type of flow unit identified based on the FZI index can effectively reflect the reservoir characteristics to a degree.

Combined with the analysis of the characteristics of the relative permeability curve of the divided flow unit types, the relative permeability endpoints and curve shapes of different types of flow units were different (Figure 5). Moreover, the division of flow units can well reflect the differences of reservoir seepage characteristics. From type I flow unit to type IV flow unit, the saturation of irreducible water and residual oil increased, and the interval of two-phase coinfiltration zone decreases (Table 1).

3.1.2. Dynamic Parameters of Flow Unit Evaluation. Difficulties in the dynamic evaluation of flow unit are in selecting dynamic parameters. Through comparing analysis and test

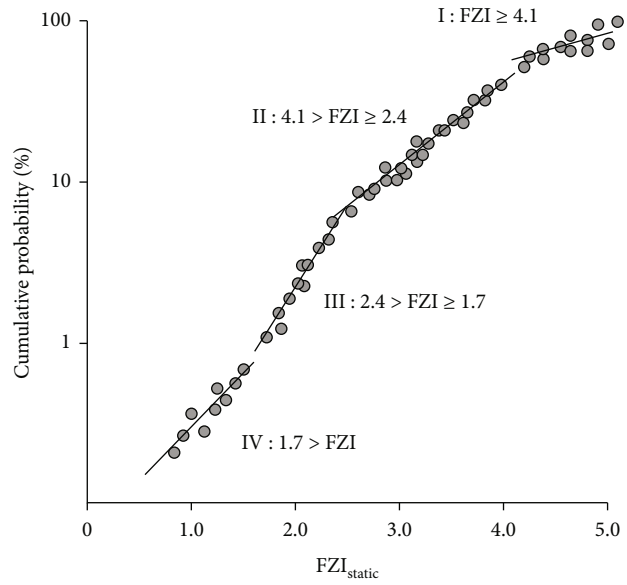

Figure 2: FZI static cumulative probability curve.

data of over ten coring wells in three periods within the study area, it is observed that with the development of water injection, shale content, and carbonate content decrease, porosity increases slightly, and permeability greatly changes (Table 2).

However, numerous previous experimental results show that during water injection development, an increase in reservoir water flow increased the porosity and permeability of the reservoir [39–43]. Hence, the W_T of the reservoir induces a change in the reservoir to a degree. Calculating the W_T amount of each flow unit and establishing the relationship between the W_T amount and the characteristics of the flow unit is the key to evaluating the dynamic parameter research of the flow unit.

Using the FZI as the static parameter of flow unit evaluation, in order to achieve the water injection splitting based on flow unit classification, the correlation between reservoir water absorption capacity and FZI was determined through the water injection profile of test data. Moreover, the FZI was introduced into the reservoir engineering method to achieve the water injection splitting of the reservoir. Through the △FZI of a similar reservoir in pairs of subwells drilled in different periods, the relationship between W_T and △FZI was fitted. Furthermore, the △FZI induced by water injection was combined with the static parameters of flow unit evaluation (FZI static) as the dynamic parameters of flow unit evaluation (FZI dynamic; Formula (2)).

$$\mathrm{FZI(dynamic)} = \mathrm{FZI(static)} + \triangle\mathrm{FZI}. \quad (2)$$

Since the W_T data is time-continuous dynamic data, theoretically, the (FZI dynamic) performance in different periods can be calculated following △FZI to study the dynamic change characteristics of the flow unit during water injection development.

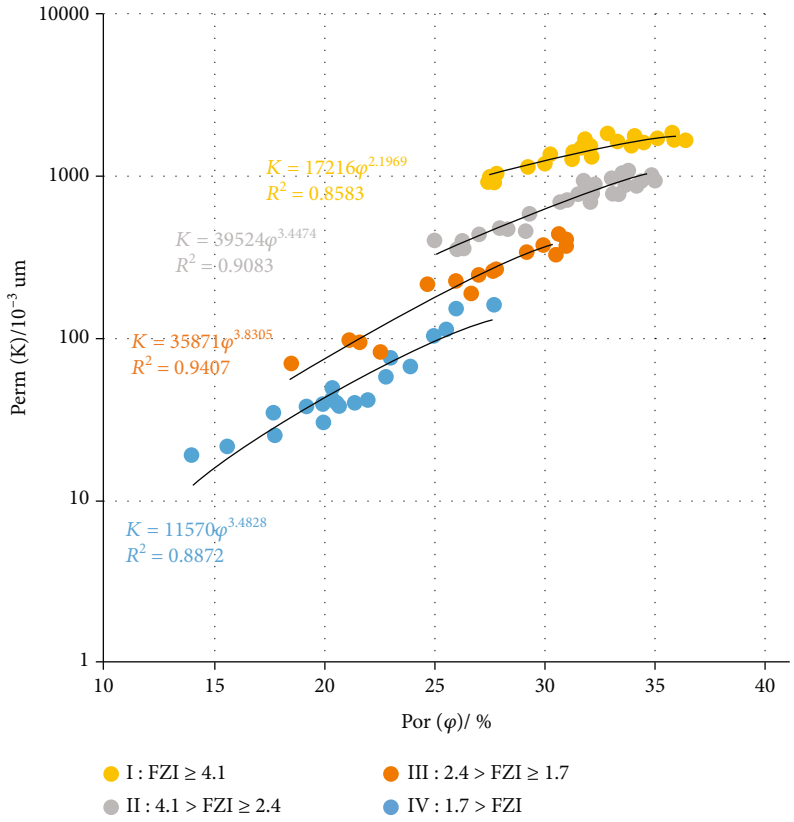

Figure 3: Relationship between porosity and permeability of different types of flow units.

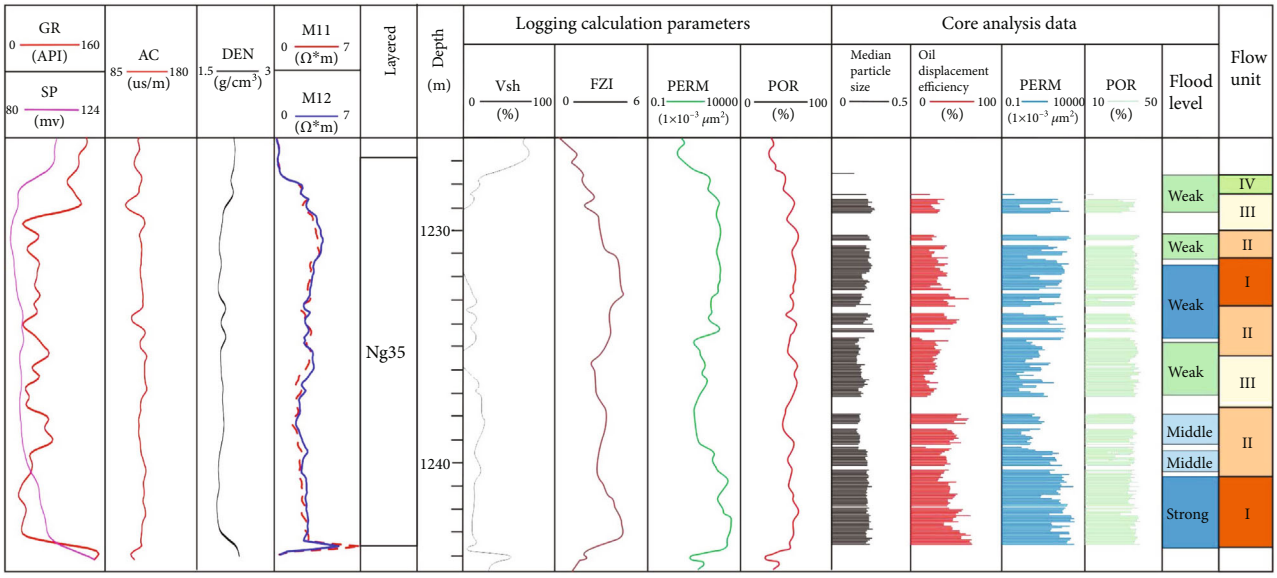

Figure 4: Comprehensive column division of flow unit in corewell.

(1) Water Injection Splitting Method. In the dynamic data, the water flow of each flow unit of the water injection well and oil production well was difficult to measure. Consequently, it cannot be directly used to calculate the calculation of cumulative water injection. To obtain the cumulative water injection data of each flow unit, the water injection splitting method should be studied to calculate the internal water flow of each flow unit and obtain the cumulative water injection.

The influence of reservoir flow unit characteristics could not be overlooked in water injection splitting. Moreover, the relative water injection and water absorption intensity in dynamic monitoring data reflected the water absorption

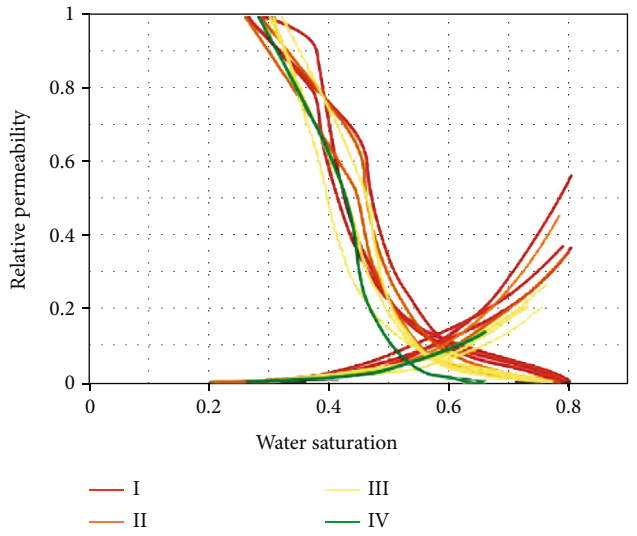

Figure 5: Characteristics of phase permeability curves of different types of flow units.

capacity of different reservoir parts and the difference in reservoir flow units. According to the correlation analysis results of 81 water absorption profiles of test data points of FZI and water absorption intensity and relative water injection of 18 wells, the correlation coefficient between water absorption intensity per unit thickness and FZI was 0.7608 (Figure 6(a)). Furthermore, the correlation coefficient between relative water injection per unit thickness and FZI was 0.845 (Figure 6(b)). This shows that the FZI, as the basis for the division of flow units, reflects the water absorption capacity of the reservoir to a degree.

In order to clarify the relationship of water flow between water injection wells and oil production wells, based on the theory of seepage mechanics and reservoir engineering, the discrimination model of seepage resistance under the constraint of injection production relationship is established by using Darcy formula and hydropower similarity principle.

According to the magnitude of seepage resistance, the water flow on each injection production relationship is analyzed with reference to parameters such as interwell flow unit type, effective thickness, flow zone index, and well spacing. It is comprehensively summarized into three modes: plane series, plane parallel, and vertical multilayer parallel (Figure 7).

Step 1. Calculate the seepage resistance of layer I of water injection well and well J of affected well. Taking the water injection well as the center, and calculate the seepage resistance coefficient of each small layer in the oil well direction around the water injection well:

$$R_{ij} = \frac{2L_{ij}}{(H_i + H_j)^2} \times \left(\frac{H_i}{FZI_i} + \frac{H_j}{FZI_j}\right). \tag{3}$$

Step 2. Calculate the total plane seepage resistance of layer I of water injection well (hydropower similarity principle):

$$R_{\text{plane}(i,j)} = \frac{1}{\left(\sum_{j=1/R_{ij}}^{n}\right)}. \tag{4}$$

Step 3. Calculate the water injection proportion coefficient from the i-th layer of water injection well to the j-th oil well affected:

$$\lambda_{\text{plane}(i,j)} = \frac{R_{\text{plane}(i,j)}}{R_{(i,j)}}. \tag{5}$$

Step 4. Calculate the total resistance of water injection well:

$$R_{\text{Total resistance}} = \frac{1}{\left(\sum_{i=1/R_{\text{plane}(i,j)}}^{n}\right)}. \tag{6}$$

Step 5. Calculate the split water injection proportion coefficient of layer I of water injection well:

$$\lambda_{\text{vertical}(i)} = \frac{R_{\text{Total resistance}}}{R_{\text{plane}(i,j)}}. \tag{7}$$

Step 6. Calculate the water injection volume from the water injection well to the i-th layer:

$$W_i = \lambda_{\text{vertical}(i)} \times Q_w. \tag{8}$$

Step 7. Water injection from the i-th layer of water injection well to the j-th effective oil well:

$$W_{ij} = \lambda_{\text{plane}(ij)} \times W_i. \tag{9}$$

In the formula:

(i) $R_{ij} - ij$. Resistance between two points (m^3/PAS)

(ii) $L_{ij} - ij$. Well spacing between two points (m)

(iii) H. Thickness of flow unit (m)

(iv) FZI. Flow zone index

(v) $R_{\text{plane}(i,j)}$. Total plane seepage resistance of layer i of water injection well

(vi) $\lambda_{\text{plane}(i,j)}$. Proportional coefficient of water injection from the i-th layer of water injection well to the j-th effective oil well

(vii) $R_{\text{Total Resistance}}$. Total resistance of water injection well

(viii) $\lambda_{\text{vertical}(i)}$. Proportional coefficient of split water injection in layer i of water injection well

(ix) W_i. Water volume from water injection well to layer i

(x) W_{ij}. Water quantity injected into the j-th effective oil well in the i-th layer

Table 1: Statistics of phase permeability parameters of different types of flow units.

Experimental parameters	Type I flow unit	Type II flow unit	Type III flow unit	Type IV flow unit
Swi (%)	26.5	27.3	30.8	35.2
Sor. (%)	19.9	21.3	24.4	25.3
Two phase coinfiltration zone (%)	53.6	51.4	44.8	39.5
Isoosmotic point water saturation (%)	58	58.3	57.7	56.9
Isoosmotic point infiltration	0.108	0.086	0.059	0.054
Number of samples, block	3	3	3	1

Table 2: Statistics of reservoir characteristics in different periods.

Period	Porosity (%)	Permeability ($\times 10^{-3}$ μm^2)	Carbonate (%)	Mud content (%)	Oil saturation (%)
Initial stage	32.3	1037	2.16	11.2	61.8
Medium high water cut period	33.6	1645	1.78	9.6	52.9
High water cut period	34.1	3512	1.27	6.97	45.4

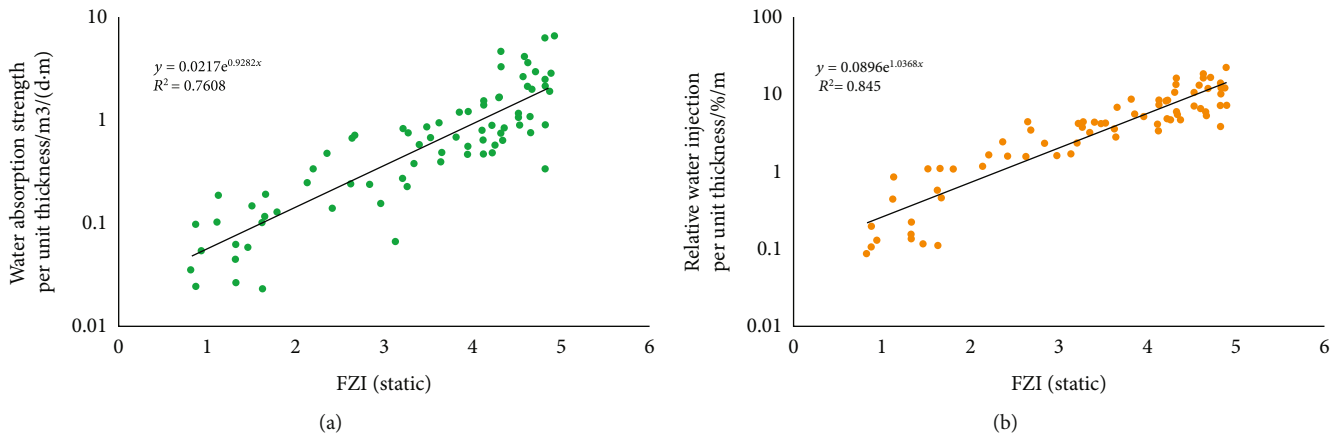

Figure 6: Correlation analysis between FZI and water absorption profile data. (a) The relationship between flow band index and water absorption strength. (b) Relationship between flow zone index and relative water injection per unit thickness.

According to this water injection splitting method, the water injection volume of each water injection well in the direction of surrounding oil wells and the cumulative water injection volume (W_T) of each flow unit can be calculated. The water injection volume splitting of different flow units in each direction can be achieved by combining the correlation between the FZI and water absorption capacity confirmed above.

(2) Calculation of Flow Zone Index Change (△FZI). From the above analysis, △FZI is the key parameter for determining the dynamic parameters (FZI dynamics) of the flow unit evaluation. For the subwells, the well spacing was relatively close, and the original reservoir flow unit types had similar characteristics. Suppose the drilling time of the two wells differed, the later drilling data could be used to evaluate the flow unit change characteristics after the first drilling and water injection development (Figure 8(a)). Furthermore, the later drilling data could be used to calculate the △FZI. There are eight pairs of subwells in the upper section of Guanguan in the study area. The drilling time difference ranges from 39 to 367 months, and the W_T difference ranges from 2×10^{-3} μm^2 – 274×10^{-3} μm^2. Through the correlation analysis between the W_T and the △FZI among subwells, it is observed that the W_T of different types of flow units has a good correlation with the △FZI (Figure 8(b)). Among them, type I and II flow units have better reservoir characteristics, and the larger the water injection volume, the greater the increase of the FZI. Conversely, type III and IV flow units have a lower increase in the FZI with an increase in water injection volume.

Following the analysis above, the fitting relationship between the W_T of four types of flow units and the △FZI between pairs of subwells can be obtained. Therefore, the △FZI can be estimated by the size of W_T in the flow unit.

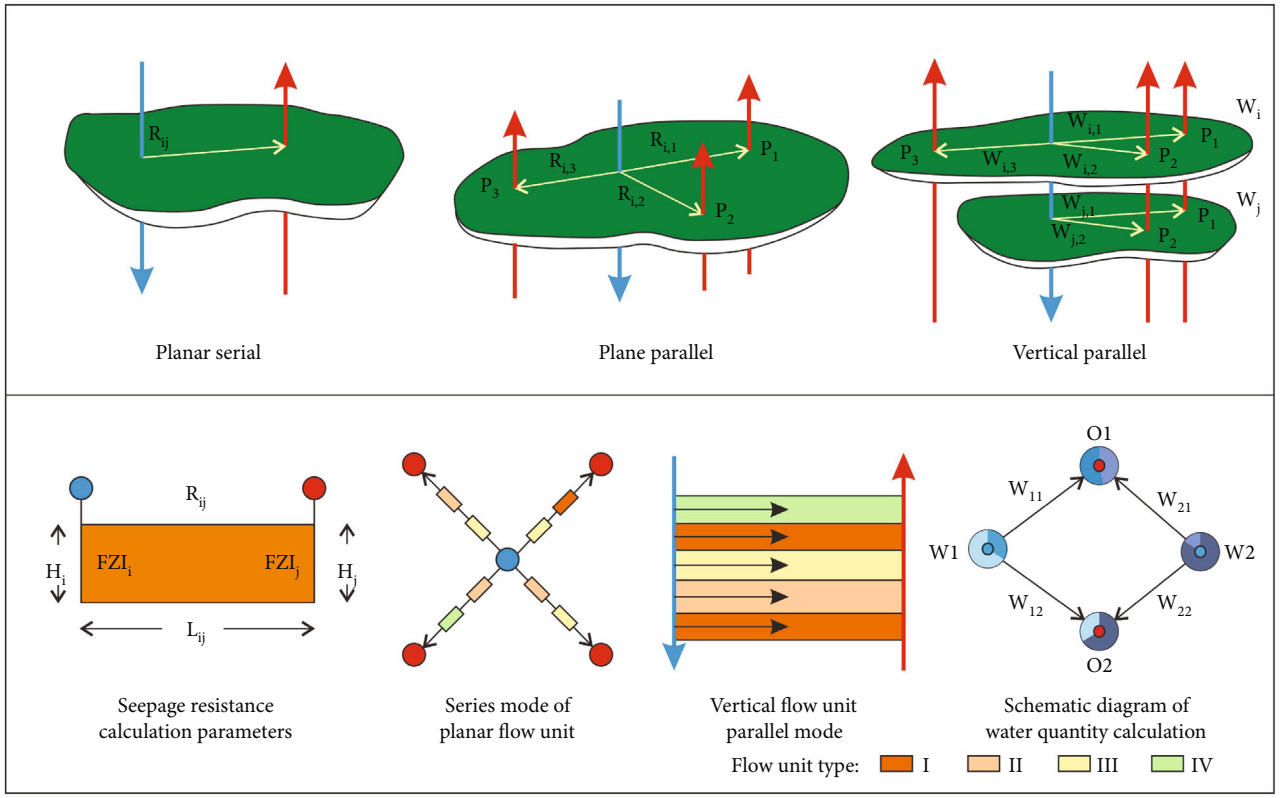

Figure 7: Discrimination mode of seepage resistance under injection production correspondence.

Hence, the dynamic parameters of flow unit evaluation (FZI dynamic) can be determined.

$$(\mathrm{i})\triangle \mathrm{FZI} = 0.3732 \ln (W_t) - 0.3635, \quad (10)$$

$$(\mathrm{ii})\triangle \mathrm{FZI} = 0.2909 \ln (W_t) - 0.3051, \quad (11)$$

$$(\mathrm{iii})\triangle \mathrm{FZI} = 0.1148 \ln (W_t) - 0.0288, \quad (12)$$

$$(\mathrm{iv})\triangle \mathrm{FZI} = 0.0272 \ln (W_t) - 0.0204, \quad (13)$$

Furthermore, through the above fitting formula, the FZI of flow unit in different periods was predicted. Verified through the FZI calculated by postdrilling, the coincidence rate reached 88.3%. Therefore, this method can predict the change in reservoir flow units caused by water injection development.

4. Results

4.1. Flow Unit Evaluation. Figure 9 shows that the combination of dynamic and static evaluation of the reservoir flow unit can be conducted using FZI static and FZI dynamic parameters to achieve the transformation from instantaneous characteristic representation of the flow unit to realistic characteristic representation.

Figure 9(a) is the plan distribution of flow units of the Ng35 layer in 1983, drawn using FZI static as the evaluation parameter, while Figure 9(b) is the plan distribution of flow units of the Ng35 layer in 2021, drawn using FZI dynamic as the evaluation parameter. Figure 9 shows that the plane distribution of flow units evaluated by FZI static and FZI dynamic parameters is different. Conversely, the range of type I and II flow units in Figure 9(b) is significantly larger. This shows that water injection development has a positive trend of improving the type of flow units, and it corresponds with the above recognition.

At different times, there were 653 water injection profiles of logging data from 44 wells in the study area. The overall error rate was below 8% by verifying the calculation results of the dynamic flow unit using the relative water injection at different times in a single well. Therefore, the change in the relative water injection in the water injection profile of test data confirmed the rationality of the dynamic static combination evaluation of the flow unit (Figure 10). With the continuous development of water injection, the FZI rose, and the corresponding relative water injection rose. However, the △FZI of different types of flow units was different, and the △FZI of type I and II flow units greatly increased.

4.2. Variation Characteristics of Flow Unit during Water Injection Development

4.2.1. Periodicity Division of Flow Unit Evolution. The variation characteristics of the flow unit are closely related to the cumulative water injection. They are affected by the improvement of well patterns and the process of water injection development. According to the characteristics of well pattern infilling and adjustment measures of large-scale water injection development in the study area, the

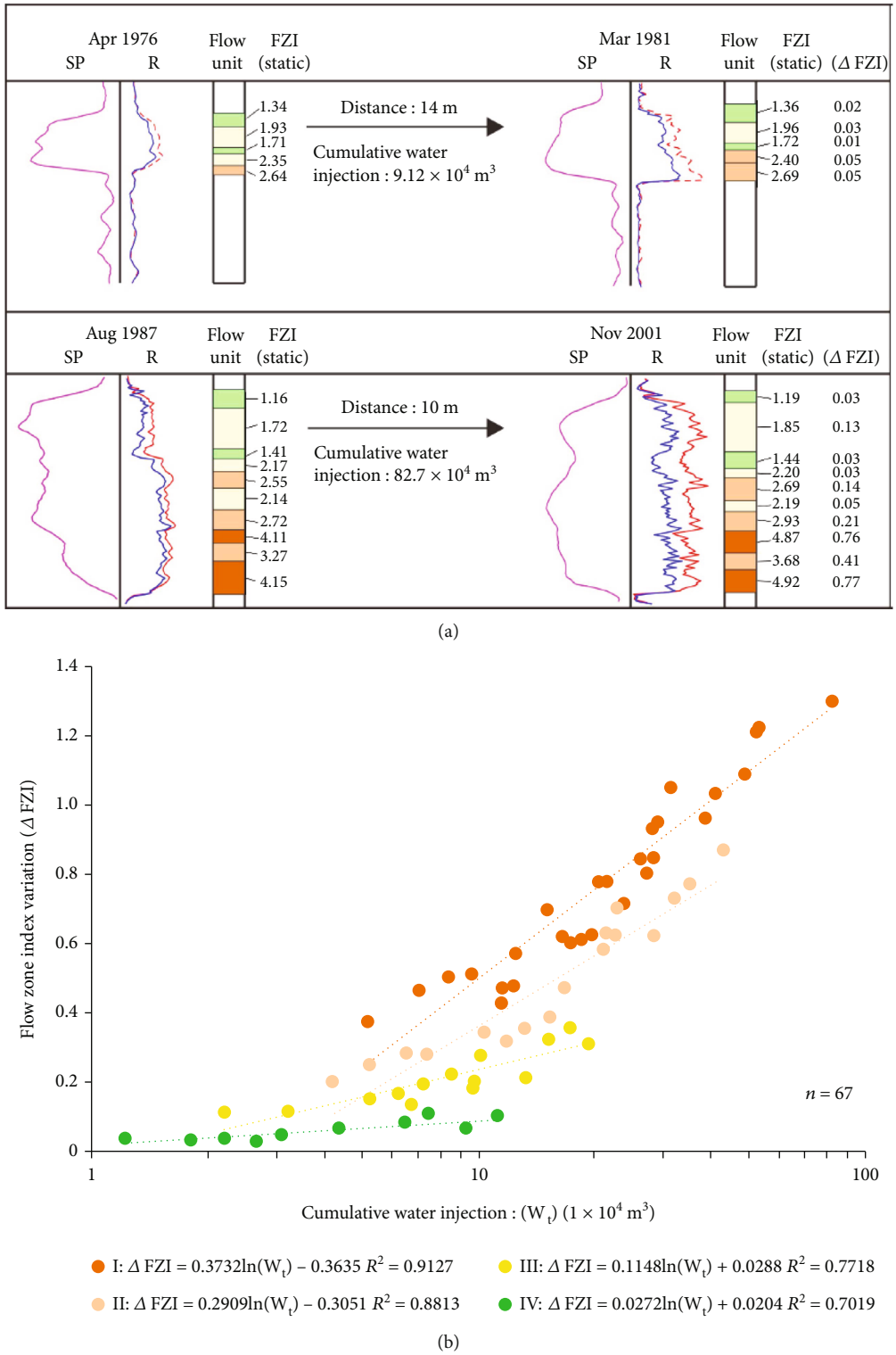

Figure 8: Relationship between cumulative water injection of subwells and FZI variation. (a) Flow unit characteristics of subwells. (b) Relationship between flow zone index change and cumulative water injection.

development process of the Ng35 layer was divided into five periods (Table 3) to study the dynamic change characteristics of the reservoir flow unit during water injection development following the production characteristic curve of Ng35 layer (Figure 11), and the five periods visibly differed in production characteristics, which represented the change characteristics of flow units discussed.

4.2.2. Plane Variation Characteristics of Flow Unit. FZI (static) and FZI (dynamic) were used to evaluate the flow

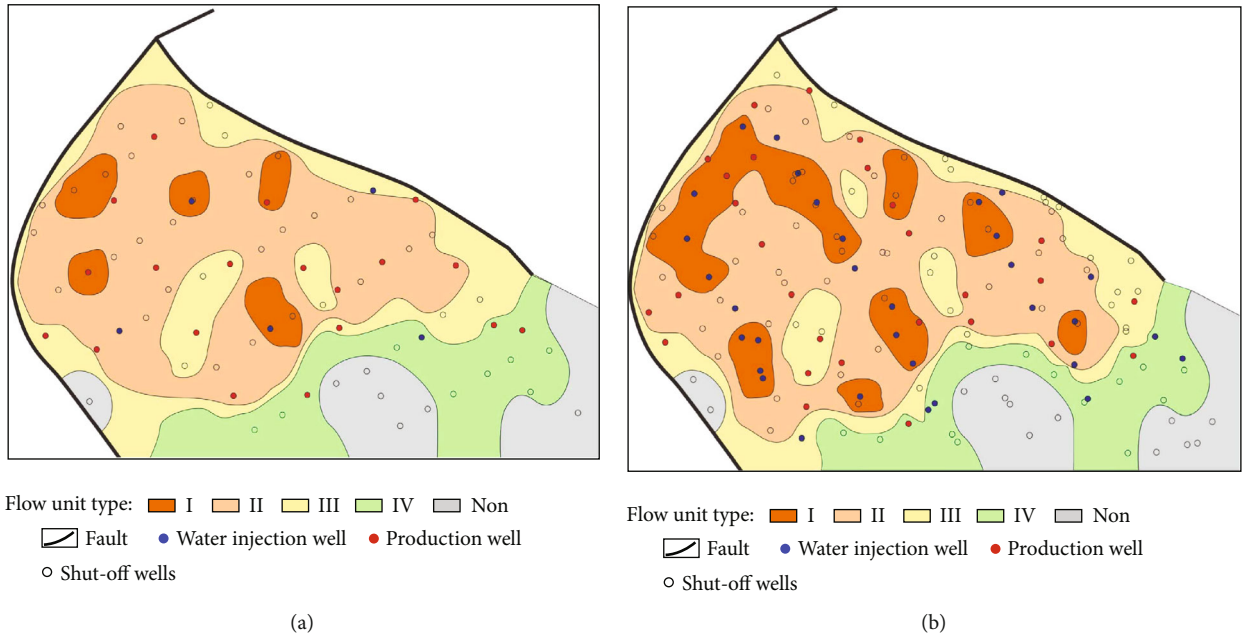

Figure 9: Evaluation diagram of dynamic static-combined flow unit on Ng35 floor. (a) FZI static flow unit layout plan (1983). (b) FZI dynamic flow unit layout plan (2021).

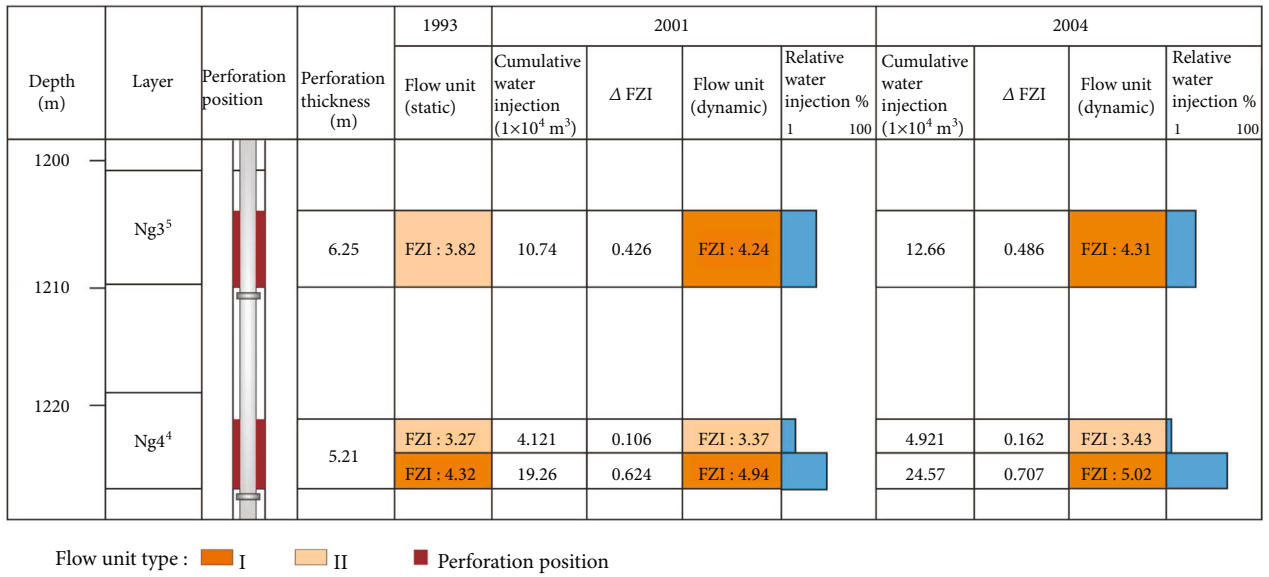

Figure 10: Test data of water absorption profile.

Table 3: Division of development period of the study area.

Period	Start and end date	Number of wells/well	Water injection well/well	Period characteristics
Period 1	1973 ~ 1983.5	75	5	At the initial stage of production, the water injection time is short, and most of them are from oil production to water injection, with small water injection volume.
Period 2	1983.5 ~ 1991.4	121	23	The study area has entered the period of water injection development.
Period 3	1991.4 ~ 2000.2	139	30	The moisture content reaches 90%.
Period 4	2000.2 ~ 2017.7	145	36	Before well pattern exchange.
Period 5	2017.7 ~ today	145	24	The well pattern streamline changes by 40° as a whole.

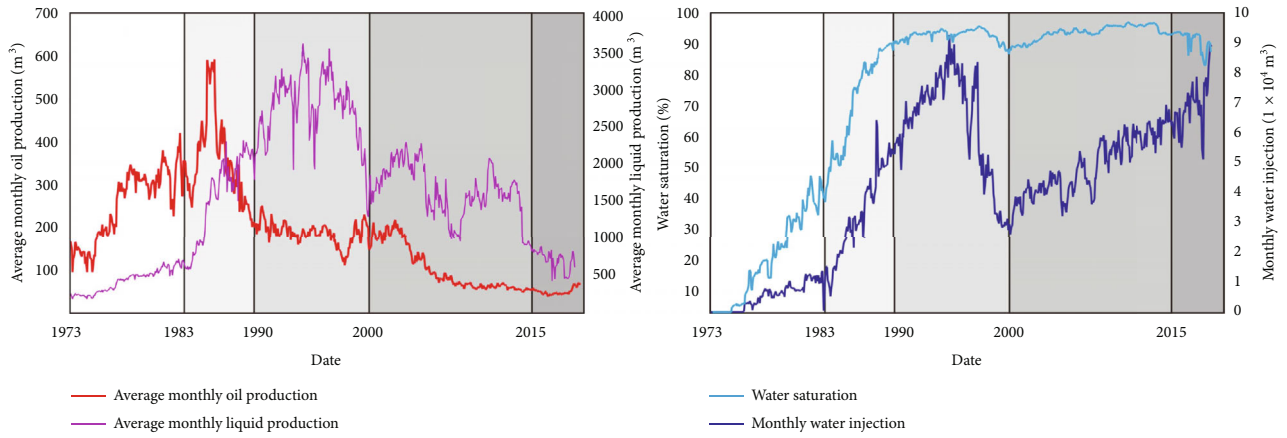

Figure 11: Overall production characteristic curve of block.

units of the Ng35 layer in five periods, draw the plane distribution map of flow units in five periods (Figure 12), and study the dynamic change characteristics of reservoir flow units during water injection development.

(1) Plane Distribution Characteristics of Flow Units in Different Periods. Period 1: The type of flow units was mainly Type II, Type I flow units were locally developed, and Type IV flow units were mostly in the south (Figure 12(a)). This period was the early stage of oilfield production, with low water injection, high oil production, and average water cut below 40%, which reflected the characteristics of the initial reservoir flow unit in the study area to a degree.

(i) *Period 2*. The proportion of type I flow units increased (Figure 12(b)), and the water accumulated in the layer (241.4×10^4 m^3); the liquid production increased greatly, and the formation of water cut increased significantly. The change in flow unit type in this period was mainly the change of flow unit distribution characteristics induced by well pattern infilling

(ii) *Period 3*. The W_T was about 1043.3×10^4 m^3; the moisture content was greater than 90%. Affected by a large amount of water injection development in the northwest of the study area, local type II flow units were transformed into type I flow units (Figure 12(c))

(iii) *Period 4*. The monthly water injection decreased; the W_T was about 2075×10^4 m^3. The development time was long, and the WT was large. The study area entered a high water cut period. Affected by long-term water injection, the distribution pattern of type I flow units was gradually consistent with the direction of the water injection well network (Figure 12(d)). Some type III and type IV flow units in the southeast were injected into the area as water injection wells, resulting in large water flow, increased FZI, and increased level of flow units

(iv) *Period 5*. During this period, the well pattern streamline was adjusted, the streamline angle changed by about 40°, the distribution position of water injection wells changed greatly, and the change of water injection concentration resulted in a change in type I flow unit distribution shape affected by a change in well pattern streamline (Figure 12(e))

(2) Control Factors of Plane Change of Flow Unit. After a long time of water injection development, the proportion of type I and type II flow units increased, and the distribution trend of flow units was roughly the same as that of production wells. Affected by water injection, the type of flow unit where production water injection wells were located changed greatly, and most of them were transformed into type I flow units. After well pattern exchange, the distribution trend of the flow unit changed with a change in the streamlined direction of the production well row. The overall change of type IV flow units was small, indicating that the seepage capacity of low-level flow units was weak, and the change of reservoir characteristics was small in the process of injection production development. Simultaneously, due to the water injection wave and its influence, the types of flow units in the central region changed relatively greatly. Type I flow units significantly increased compared with the initial stage of development, forming the main high water consumption zone on the plane. This region absorbed most of the water injection, has high liquid production, high water content, and low water drive efficiency in other regions. The change in different types of flow units was mainly controlled by the injection production well pattern and cumulative water injection.

4.3. Relative Variation Characteristics of Interlayer Flow Units. The stable-developed interlayer between small layers ensures the mining independence of each layer. During combined injection and production, the difference in flow unit caused uneven water absorption between layers. Combined with the change characteristics of the flow unit, the change of interlayer interference was analyzed, mainly manifested in two characteristics.

4.3.1. Increase Type Change. These characteristics were mainly reflected in the combined injection and production

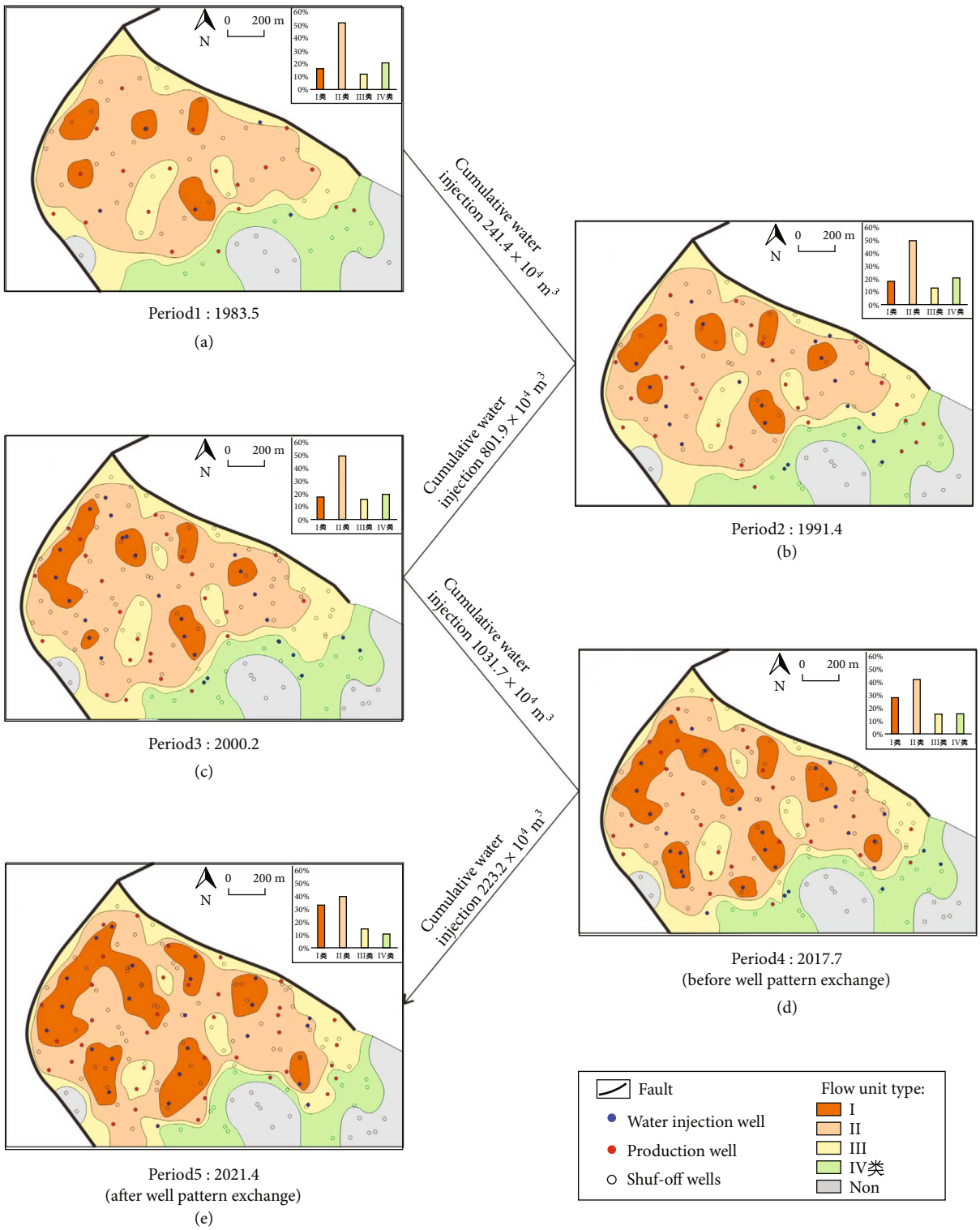

Figure 12: Plane distribution of various types of flow units in different periods.

wells. The water absorption intensity of the reservoir was exponentially related to the FZI; that is, the water absorption capacity of the index flow unit of the high flow zone was much greater than that of the index flow unit of the low flow zone. With the long-term combined injection and production, the difference between the reservoirs further expanded, increasing the difference in water absorption intensity, interlayer interference enhancement. The well where NG35 and NG44 developed a set of thick oil layers (Figure 13) was drilled in 1988. They were initially used as production wells and then converted to water injection wells. In the water injection profile test conducted in 2000, the relative water

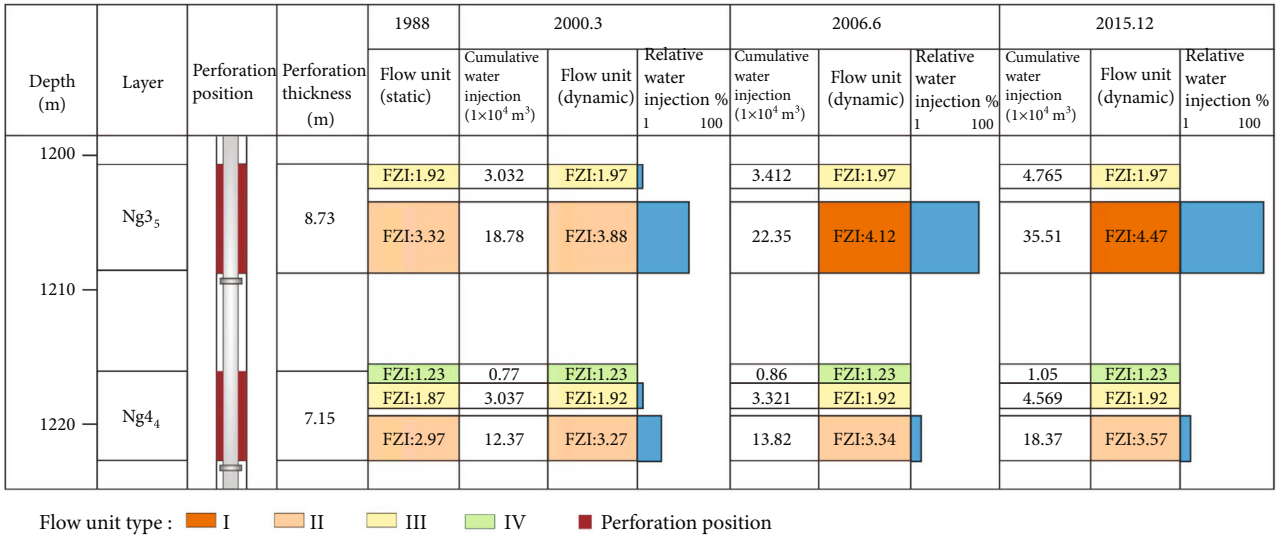

Figure 13: Test results of increasing interlayer differential water absorption profile.

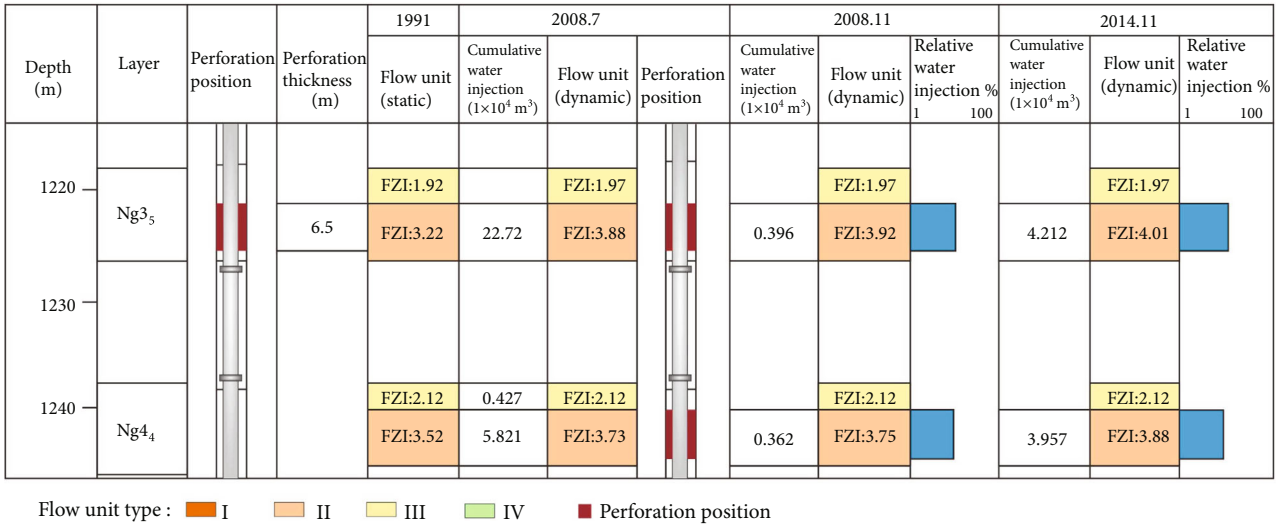

Figure 14: Test results of amplitude reducing interlayer differential water absorption profile.

injection ratio of the two layers was 1.77, and the water absorption difference between layers was small. In the test in 2006 and 2015, the relative water injection ratio was 4.26 and 13.2, respectively. The long-term water injection development enhanced the reservoir heterogeneity and formed an increasing interlayer difference.

4.3.2. Amplitude Reduction Type Change. These characteristics were mainly the reduction of the interlayer difference caused by single-layer development. For example, the perforation position was in the small upper layer. The lower small layer was not perforated, which induced an increase in the FZI and a decrease in the difference between the FZI and the lower small layer in the lower low-level flow unit of the small upper layer under the influence of water injection development. Subsequently, the difference in relative water injection volume between layers in the subsequent process of combined injection and production became smaller. When the well was drilled in 1991, only the upper layer of the NG35 was perforated at the initial stage (Figure 14), and the FZI was lower than that of Ng44. In 2008, the W_T of Ng35 was 22.72×104 m^3, the Ng44 layer was not on the main injection production line, the water flow was small, and the increase in FZI was much less than that of Ng35, subsequently, the well-patched Ng44 layer. Combined with the analysis of later water injection profile of test results, the difference of relative water injection between layers was small due to a decrease in index difference of interlayer flow zone. This feature was the amplitude-reducing interlayer difference induced by the imperfect injection production relationship.

In general, long-term water injection development will increase the FZI of the reservoir. The difference in water

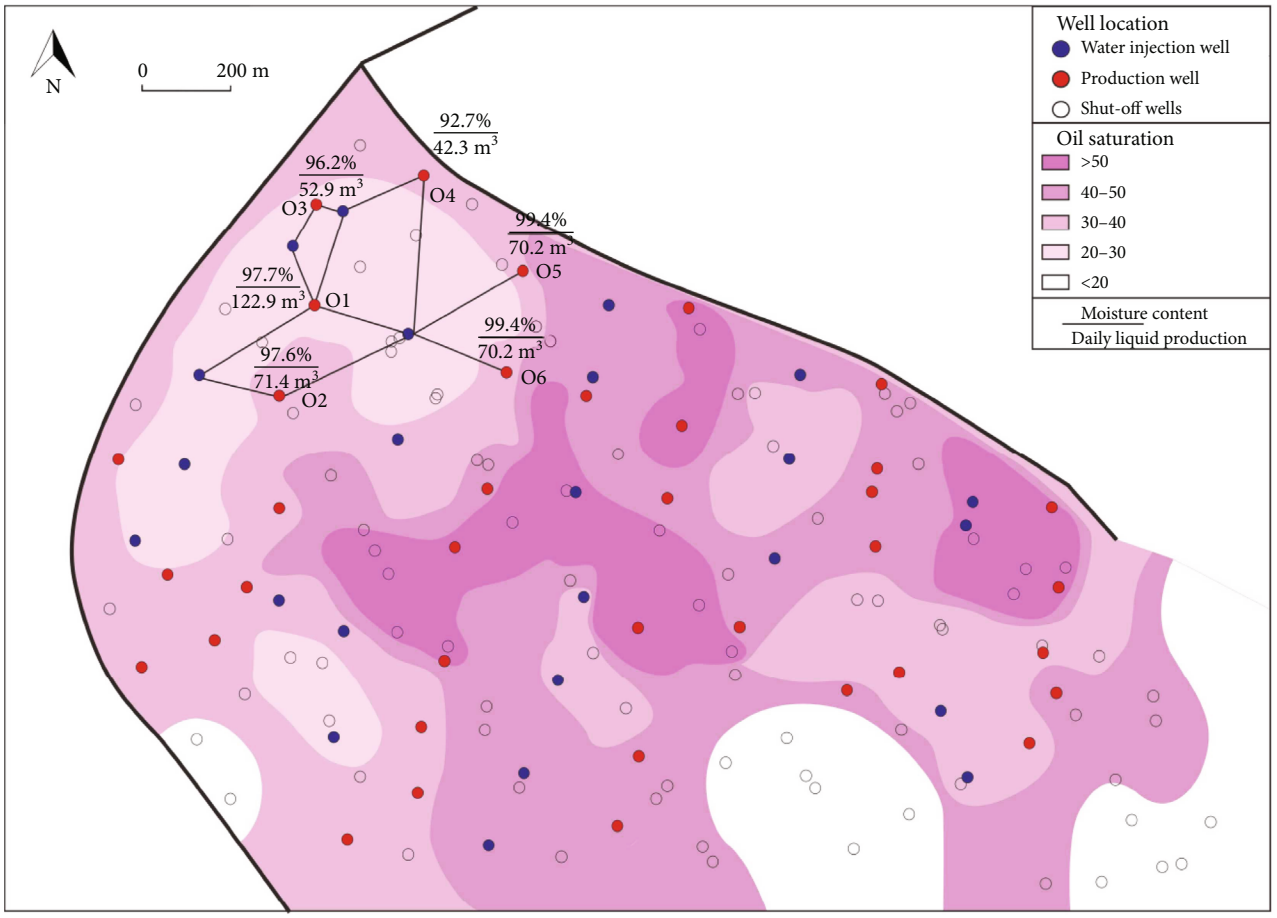

Figure 15: Oil saturation distribution plan of Ng35 layer.

injection volume will induce a difference in the change in the FZI of the reservoir and then affect the water injection development of the reservoir.

5. Discussion

5.1. Production Problems under Flow Unit Control. These characteristics were mainly the reduction of the interlayer difference caused by single-layer development. For example [44, 45], the perforation position was in the small upper layer. The lower small layer was not perforated, which induced an increase in the FZI and a decrease in the difference between the FZI and the lower small layer in the lower low-level flow unit of the small upper layer under the influence of water injection development. Subsequently, the difference in relative water injection volume between layers in the subsequent process of combined injection and production became smaller. When the well was drilled in 1991, only the upper layer of the NG35 was perforated at the initial stage (Figure 14), and the FZI was lower than that of Ng44. In 2008, the W_T of Ng35 was $22.72 \times 10^4\ m^3$, the Ng44 layer was not on the main injection production line, the water flow was small, and the increase in FZI was much less than that of Ng35, subsequently, the well-patched Ng44 layer. Combined with the analysis of later water injection profile of test results, the difference of relative water injection between layers was small due to a decrease in index difference of interlayer flow zone. This feature was the amplitude-reducing interlayer difference induced by the imperfect injection production relationship.

The change in injection production streamlined angle implemented in the study area in 2017 [37] can alleviate the defects, such as low production efficiency induced by reservoir differences and improve oil recovery to a certain extent. However, due to the change of flow unit type, from the research results and water injection profile of test results, there were still many changes in the injection production well pattern streamline, and the injection production relationship was located in high-level flow units. Local water absorption is too serious. According to the comprehensive analysis of production data, oil saturation plan, and dynamic flow unit distribution characteristics (Figure 15), the overall oil saturation in the well pattern area in the north of the study area was low, and the plane heterogeneity was serious. Several water injection wells were type I flow units, and the only oil well in the nearby oil wells was type I flow unit. Since the well pattern was exchanged, the average daily liquid production is $122.9\ m^3$, much higher than other oil wells. The distribution of type I flow units induced the formation of dominant seepage channels between this well and nearby

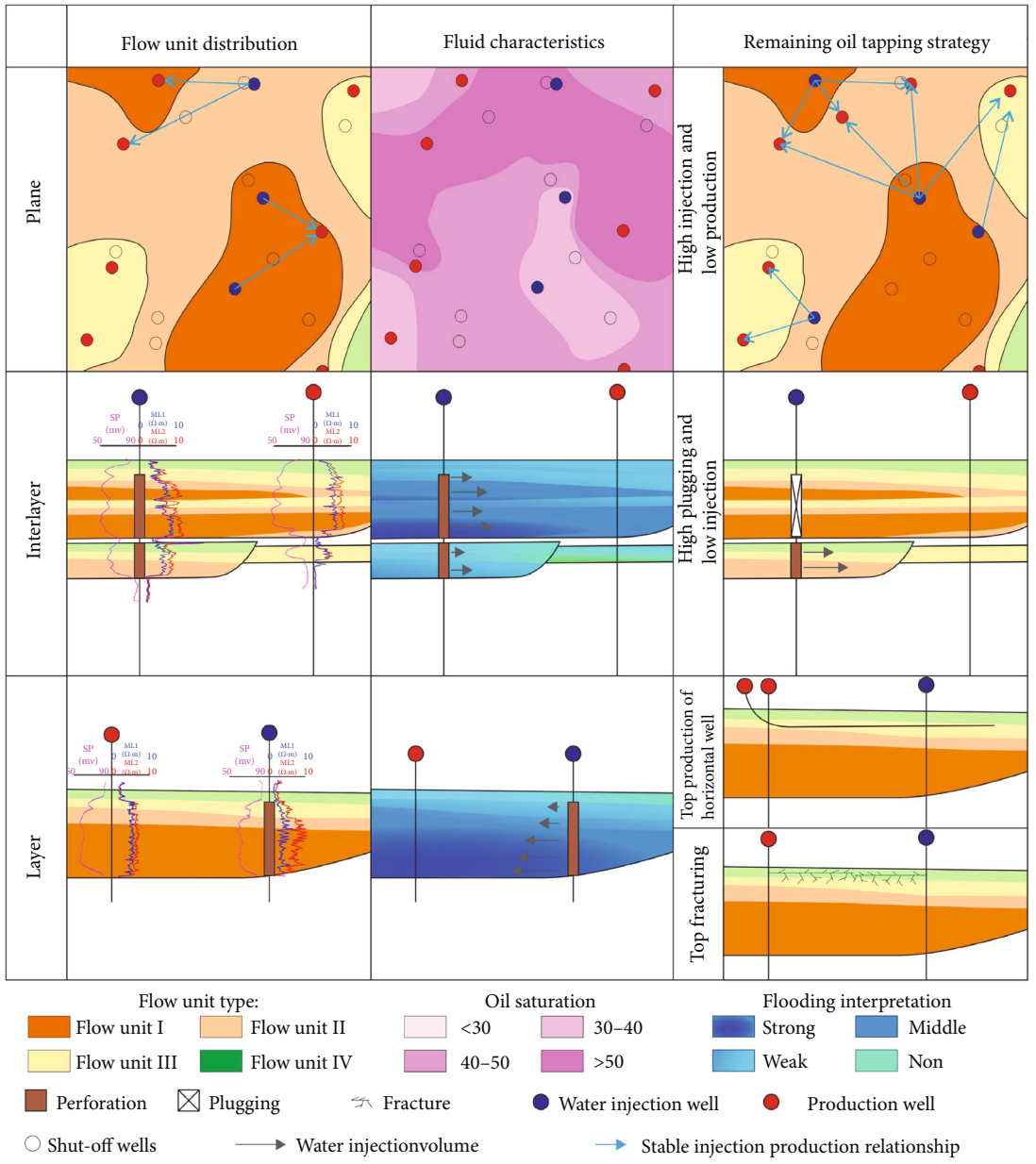

Figure 16: Different types of remaining oil and their potential tapping strategies

water injection wells. This induced low injection and production efficiency of nearby oil wells and difficulties in tapping the potential of the remaining oil.

The overall water cut in the study area is high. However, the middle part still has high oil saturation, indicating that the difference of flow units in the layer is also huge, and the heterogeneity was strong. Type III, IV, and some type II flow units still have high reserves. Therefore, the reason for tapping the potential of the remaining oil in high water cut reservoirs was to adjust the well pattern, establish a new injection production relationship, and adjust the development mode of a plane, an intralayer, and an interlayer in order to avoid the extreme water consumption of dominant seepage channels.

5.2. Remaining Oil Distribution under the Control of the Flow Unit and Its Potential Tapping Strategy. According to the distribution characteristics of flow units, oil saturation, and water flooding results in the study area, a strategy for tapping the remaining oil potential of the plane [46, 47], interlayer, and intralayer based on the distribution characteristics of dynamic flow units was proposed (Figure 16).

5.2.1. Potential Tapping Strategy of Plane Remaining Oil. Most of the plane remaining oil was formed due to the imbalance of water drive efficiency induced by the plane difference of reservoir flow units. Presently, under the well pattern state, two water wells and one oil well in the middle are located within the distribution range of type I flow units,

forming an advantageous injection production channel with stable strength. Due to the difference in flow unit types, the water flow is small for other oil wells, and the displacement is uneven. Therefore, according to the distribution characteristics of dynamic flow units, the strategy of "high injection and low production" can be adopted; that is, type I flow unit wells are used as the main water injection wells, and other types of flow units are used as production wells. This well pattern feature can avoid the formation of extremely advantageous seepage channels to a degree, improve injection and production efficiency, and tap the potential of remaining oil.

5.2.2. Potential Tapping Strategy of Interlayer Remaining Oil. During combined production, there were large differences in interlayer flow units, resulting in very small overall relative water absorption and low displacement efficiency. This feature often induced extremely rich residual oil content and low water flooding degree in the horizon with small relative water absorption. For this feature, the method of "high plugging and low injection" can be used for production, that is, blocking the hole for the horizon with great water absorption and focusing on exploiting the horizon with relatively small water absorption. The previous research confirmed that the development of water injection increases the FZI and water absorption capacity of the reservoir. Furthermore, when the difference between the FZIes of the two layers is small, joint injection and production can improve the oil displacement efficiency.

5.2.3. Potential Tapping Strategy of Remaining Oil in the Formation. The remaining oil in the layer is mostly rhythmic characteristics of the reservoir, resulting in a high FZI at the bottom of the sand body, serious water flooding, low water flooding level or no water flooding at the top of the sand body, and relative enrichment of the remaining oil. Regarding this feature, the remaining oil potential can be tapped using centralized production of horizontal well drilling in the top sand body or fracturing at the top of the sand body to increase the fluid flow capacity of the reservoir.

6. Conclusions

(1) Using the FZI as the static parameter of flow unit evaluation, four types of flow units were divided: type I flow unit, $FZI \geq 4.1$; type II flow unit, $4.1 > FZI \geq 2.4$; type III flow unit, $2.4 > FZI \geq 1.7$; type IV flow unit, $1.7 > FZI$. The reservoir porosity and permeability characteristics of different types of flow units are highly correlated

(2) To achieve water injection splitting based on flow unit classification, the correlation between reservoir water absorption capacity and FZI was determined through the water injection profile of test data. Subsequently, the flow zone index was introduced into the reservoir engineering method to split reservoir water injection. The relationship between W_T and $\triangle FZI$ was fitted through pairs of wells drilled in different periods. The $\triangle FZI$ caused by water injection volume was combined with the static parameters of flow unit evaluation (FZI static) as the dynamic parameters of flow unit evaluation (FZI dynamic)

(3) The evolution results of reservoir flow units in different periods show that water injection development improves the flow zone index, but an increase in the same water injection for type I and II flow units is much greater than that for type III and IV flow units. Hence, water injection development will further enhance the heterogeneity of the reservoir. The change in different types of flow units is mainly controlled by the injection production well pattern and W_T. The relative variation characteristics of two kinds of interlayer flow units are summarized

(4) According to the distribution characteristics of flow unit, oil saturation, and water flooding results in the study area, four remaining oil potential tapping strategies in a plane, an intralayer, and an interlayer were proposed: in the plane (high injection and low production), interlayer (high plugging and low injection), interlayer (horizontal well top production), and top fracturing

Data Availability

The data used to support the findings of this study are included within the article.

Conflicts of Interest

The authors declare that they have no conflicts of interest.

Acknowledgments

This work was financially supported by the Natural Science Foundation of Heilongjiang Province (No. YQ2019D002) and the National Natural Science Foundation of China (Nos. 41772149 and 41872158). The authors appreciate the guidance provided by the Northeast Petroleum University and Sinopec Shengli Oilfield Company.

References

[1] C. L. Hearn, W. J. Ebanks, R. S. Tye, and V. Ranganathan, "Geological factors influencing reservoir performance of the Hartzog draw field, Wyoming," *Journal of Petroleum Technology*, vol. 36, no. 8, pp. 1335–1344, 1984.

[2] M. A. Fengchun, L. I. Jincheng, W. U. Yanxiong et al., "Calculation and evaluation method of reservoir parameters in multiple oil reservoirs based on flow unit," *Geoscience*, vol. 34, no. 2, pp. 370–377, 2020.

[3] Z. Q. Chen, S. Y. Wu, and R. Baiai, "Logging evaluation for permeability of tight sandstone gas reservoirs based on flow unit classification:a case from Xujiahe Formation in Guang'an area,central Sichuan Basin," *Lithologic Reservoirs*, vol. 29, no. 6, pp. 76–83, 2017.

[4] O. M. Elnaggar, "A new processing for improving permeability prediction of hydraulic flow units, Nubian Sandstone, Eastern Desert, Egypt," *Journal of Petroleum Exploration & Production Technology*, vol. 8, no. 3, pp. 677–683, 2018.

[5] S. N. Al-Jawad and A. H. Saleh, "Flow units and rock type for reservoir characterization in carbonate reservoir: case study, south of Iraq," *Journal of Petroleum Exploration and Production Technology*, vol. 10, no. 1, pp. 1–20, 2020.

[6] J. O. Amaefule, M. Altunbay, D. Tiab, D. G. Kersey, and D. K. Keelan, "Enhanced reservoir description:using core and log data to identify hydraulic(flow)units andpredict permeability in uncored intervals/wells," in *SPE annual technical conference and exhibition*, OnePetro, 1993.

[7] J. A. Canas, Z. A. Malik, and C. H. Wu, "Characterization of flow units in sandstone reservoirs," in *Permian Basin Oil and Gas Recovery Conference*, OnePetro, 1994.

[8] I. Yusuf and E. Padmanabhan, "Impact of rock fabric on flow unit characteristics in selected reservoir sandstones from West Baram Delta offshore, Sarawak," *Journal of Petroleum Exploration and Production Technology*, vol. 9, no. 3, pp. 2149–2164, 2019.

[9] L. U. Mingzhen, L. I. Chengyan, Z. H. Xianguo, Z. Jiangtao, and S. O. Geosciences, "Evaluation and optimization of flow unit division methods," *Lithologic Reservoirs*, vol. 27, no. 1, 2015.

[10] R. Aguilera, "Flow units: from conventional to tight gas to shale gas reservoirs," in *Trinidad and Tobago Energy Resources Conference*, OnePetro, 2010.

[11] C. R. Clarkson, J. L. Jensen, P. K. Pedersen, and M. Freeman, "Innovative methods for flow-unit and pore-structure analyses in a tight siltstone and shale gas reservoir," *AAPG Bulletin*, vol. 96, no. 2, pp. 355–374, 2012.

[12] X. Z. Zhang, X. S. Wu, and Q. H. Xiong, "A new method for classifying flow units with fuzzy clustering and fuzzy recognition methods," *Journal of the University of Petroleum China*, vol. 26, no. 5, pp. 19–22, 2002.

[13] H. E. Chuanliang, K. A. Jianyun, W. A. Xin, and Z. H. Shimao, "Reservoir flow unit division based on sedimentary microfacies reservoir space type:a case of carbonate reservoir of Leikoupo Formation in Pengzhou Gas Field," *Xinjiang Petroleum Geology*, vol. 41, no. 4, pp. 435–443, 2020.

[14] J. Shang, Q. Zhang, and H. Li, "Characterization method and application of seepage units based on reservoir configuration: a case study of the Wenchang C oilfield in the Pearl River Mouth Basin," *Acta Sedimentologica Sinica*, vol. 39, no. 4, pp. 1020–1030, 2021.

[15] S. Bhattacharya, A. P. Byrnes, W. L. Watney, and J. H. Doveton, "Flow unit modeling and fine-scale predicted permeability validation in Atokan sandstones: Norcan East Field, Kansas," *AAPG Bulletin*, vol. 92, no. 6, pp. 709–732, 2008.

[16] B. Yuan, H. Zhang, Q. Ye et al., "Flow-unit classification based on compound sand-body architecture of delta and distribution pattern of remaining oil," *Acta Sedimentologica Sinica*, vol. 39, no. 5, pp. 1253–1263, 2021.

[17] Z. Fan, K. Li, J. Li, H. Song, L. He, and X. Wu, "A study on remaining oil distribution in a carbonate oil reservoir based on reservoir flow units," *Petroleum Exploration and Development*, vol. 41, no. 5, pp. 634–641, 2014.

[18] Q. Wan, S. Wu, S. Wang et al., "Multi-parameter technology on the study of flow units division and their distribution in deep-water turbidity channel reservoir," *Geological Journal of China Universities*, vol. 20, no. 2, pp. 317–323, 2014.

[19] S. Wang, Q. Wan, Y. Chen, X. Li, and J. Li, "Flow units division and their distribution law based on braided river reservoir architecture," *Petroleum Geology and Recovery Efficiency*, vol. 22, no. 5, pp. 47–51, 2015.

[20] Z. Chen, J. Lu, Y. Zhao, W. Zhang, C. Zhang, and Q. Tian, "Research on flow unit division rationality of Yan 91 oil reservoir in Yang 19 block of Suijing oilfield, Ordos Basin," *Oil & Gas Geology*, vol. 36, no. 3, pp. 497–503, 2015.

[21] G. Xiong and L. Liu, "Flow units classification based on reservoir architecture and its influence on reservoir development," *Journal of Southwest Petroleum University (Science & Technology Edition)*, vol. 36, no. 3, pp. 107–114, 2014.

[22] S. Lu, J. Li, P. Zhang et al., "Classification of microscopic porethroats and the grading evaluation on shale oil reservoirs," *Petroleum Exploration and Development*, vol. 45, no. 3, pp. 452–460, 2018.

[23] F. Gui, Z. Huang, Z. Ma, and H. Yang, "Identification and prediction of flow units using grey association cluster method," *Geoscience*, no. 3, pp. 339–344, 1999.

[24] Z. Li, M. Luo, B. Ma, and J. Liu, "Identifying the flow units with reservoir heterogeneity indicator," *Xinjiang Geology*, no. 2, pp. 203–206, 2005.

[25] Z. Dou, L. Zeng, Z. Zhang et al., "Research on the diagnosis and description of wormhole," *Petroleum Exploration and Development*, vol. 28, no. 1, pp. 75–77, 2001.

[26] L. Zeng, L. Gong, and C. Guan, "Natural fractures and their contribution to tight gas conglomerate reservoirs: a case study in the northwestern Sichuan Basin, China," *Journal of Petroleum Science and Engineering*, vol. 210, article 110028, 2022.

[27] L. Gong, S. Gao, B. Liu et al., "Quantitative prediction of natural fractures in shale oil reservoirs," *Geofluids*, vol. 2021, Article ID 5571855, 15 pages, 2021.

[28] S. Peng, Y. Shi, T. Han et al., "A quantitative description method for channeling-path of reservoirs during high water cut period," *Acta Petrolei Sinica*, vol. 28, no. 5, pp. 79–84, 2007.

[29] Q. Feng, J. Qi, X. Yin, Y. Yang, S. Bing, and B. Zhang, "Simulation of fluid-solid coupling during formation and evolution of high-permeability channels," *Petroleum Exploration and Development*, vol. 36, no. 4, pp. 498–502, 2009.

[30] C. Z. Cui, S. Li, Y. Yang et al., "Planar zoning regulation and control method of reservoir at ultra-high water cut stage," *Acta Petrolei Sinica*, vol. 39, no. 10, pp. 1155–1161, 2018.

[31] Y. H. Zhao, H. Q. Jaing, and H. Q. Li, "Identification and predictions of water injectivity for water injection channels in water injection development oilfield," *Acta Petrolei Sinica*, vol. 42, no. 8, pp. 1081–1090, 2021.

[32] Q. L. Du, "Variation law and microscopic mechanism of permeability in sandstone reservoir during long-term water flooding development," *Acta Petrolei Sinica*, vol. 37, no. 9, pp. 1159–1164, 2016.

[33] M. N. Wang, J. H. Li, Z. J. Guo, and W. Wang, "The influence of water-flooding development on reservoir properties of the no.2 member of Shahejie Formation of Tuo 30 fault block in Shengtuo oilfield," *Acta Scientiarum Naturalium Universitatis Pekinensis*, vol. 40, no. 6, pp. 855–863, 2004.

[34] C. L. Shi, F. H. Zhang, and P. Chen, "Affection of simulating water-flooding by water injection tests on reservoir properties," *Journal of Southwest Petroleum University(Science & Technology Edition)*, vol. 35, no. 5, pp. 87–93, 2013.

[35] L. Ruhao and S. Yu, "Reservoir flow units for dynamic and static combinations: case study of Neogene Guantao Formation in Block M, Gudao Oilfield," *Acta Sedimentologica Sinica*, 2022.

[36] L. X. Mu, "Stages and characteristic of reservoir description," *Acta Petrolei Sinica*, vol. 21, no. 5, pp. 103–108, 2000.

[37] H. C. Liu, "Study on response mechanism and mode of oil well after layer and well pattern interchange in Gudao Oilfield," *Petroleum Geology and Recovery Efficiency*, vol. 28, no. 5, pp. 109–115, 2021.

[38] R. Liu, Y. Sun, X. Wang, B. Yan, and H. Yu, "Characteristics of seepage barriers in fluvial reservoirs of meandering rivers and their impacts on water injection development: a case study of Neogene Guantao formation in Block M, Gudao Oilfield," *Geofluids*, vol. 2022, Article ID 8782179, 14 pages, 2022.

[39] H. Wang, M. Jiang, J. Zhang, G. Zhang, and F. Song, "Simulation on variation of physical properties in high water-cut reservoir," *Acta Petrolei Sinica*, vol. 25, no. 6, pp. 53–58, 2004.

[40] H. Li, X. W. Wang, and S. L. Liu, "Variation law of parameters of reservoir physical property in old oilfield," *Journal of Southwest Petroleum University(Science & Technology Edition)*, vol. 31, no. 2, pp. 85–89, 2009.

[41] Y. J. Zhou, W. S. Hu, Y. K. Zhang, and W. Zhang, "Law of reservoir physical property changes both before and after waterflooding—by using Es3 reservoir of South Fault Block Hu7 in Huzhuangji Oilfield for example," *Journal of Oil and Gas Technology*, vol. 32, no. 5, pp. 25–30, 2010.

[42] P. Meng and C. S. Shen, "Analysis on influence of sedimentary rhythm on water injection effect by application of water flooded layer change in twin wells," *Reservoir Evaluation and Development*, vol. 5, no. 3, pp. 33–38, 2015.

[43] C. C. Guo, "Logging comprehensive index methods of identifying relatively high-permeability zone of new well," *Well Logging Technology*, vol. 38, no. 6, pp. 755–759, 2014.

[44] Y. Li, J. Yang, Z. Pan, and W. Tong, "Nanoscale pore structure and mechanical property analysis of coal: an insight combining AFM and SEM images," *Fuel*, vol. 260, article 116352, 2020.

[45] Y. Li, J. Yang, Z. Pan, S. Meng, K. Wang, and X. Niu, "Unconventional natural gas accumulations in stacked deposits: a discussion of upper paleozoic coal-bearing strata in the east margin of the Ordos basin, China," *Acta Geologica Sinica-English Edition*, vol. 93, no. 1, pp. 111–129, 2019.

[46] J. Zhang, F. Fang, J. Wang et al., "prediction of intraformational remaining oil distribution based on reservoir heterogeneity: application to the J-field," *Advances in Civil Engineering*, vol. 2021, Article ID 8870274, 10 pages, 2021.

[47] C. Liu, W. Zhou, and J. Jiang, "Remaining oil distribution and development strategy for offshore unconsolidated sandstone reservoir at ultrahigh water-cut stage," *Geofluids*, vol. 2022, Article ID 6856298, 11 pages, 2022.